On the Explicit Formulation of Reliability Assessment of Distribution Systems with Unknown Network Topology: Incorporation of DG, Switching Interruptions, and Customer-Interruption Quantification

Mohammad Jooshaki[a,*], Matti Lehtonen[b], Mahmud Fotuhi-Firuzabad[c], Gregorio Muñoz-Delgado[d], Javier Contreras[d], José M. Arroyo[d]

[a] *Circular Economy Solutions Unit, Geologian Tutkimuskeskus (GTK), Espoo, Finland*
[b] *Department of Electrical Engineering and Automation, Aalto University, Espoo, Finland*
[c] *Electrical Engineering Department, Sharif University of Technology, Tehran, Iran*
[d] *Escuela Técnica Superior de Ingeniería Industrial, Universidad de Castilla-La Mancha, Ciudad Real, Spain*

Abstract

This paper presents an original approach for the evaluation of reliability of active distribution networks with unknown topology. Built upon novel reformulations of conventional definitions for distribution reliability indices, the dependence of system-oriented reliability metrics on network topology is explicitly formulated using a set of mixed-integer linear expressions. Unlike previously reported works also modeling mathematically the relationship between reliability assessment and network topology, the proposed approach allows considering the impact of distributed generation (DG) while accounting for switching interruptions. Moreover, for the first time in the emerging closely related literature, the nonlinearity and nonconvexity of the customer average interruption duration index are precisely characterized. The proposed mixed-integer linear model is suitable for various distribution optimization problems in which the operational topology of the network is not specified a priori. Aiming to exemplify its potential applicability, the proposed formulation is incorporated into a distribution reconfiguration optimization problem. The effectiveness and practicality of the proposed approach are numerically illustrated using various test networks.

Keywords: Active distribution networks, customer-interruption quantification, distributed generation, mixed-integer linear programming, reliability assessment, switching interruptions, unknown network topology

Nomenclature

Indices

i, j, k	Indices for feeder sections.
m	Index for paths.
n	Index for load nodes.

Sets

Π	Index set of all feeder sections.
Π^S	Subset of Π for feeder sections directly connected to substation nodes.
Ω^D	Index set of load nodes.
Ω^{DG}	Subset of Ω^D for nodes with DG units.
Ω^S	Index set of substation nodes.
$\Psi_{i,j}$	Index set of all paths between feeder sections i and j.

Parameters

D_n	Power demand at node n.
G_n	DG capacity installed at node n.
M	Sufficiently large number.
N_n	Number of customers connected to load node n.
r_i, s_i	Repair and switching times of feeder section i.
$w_C, w_D,$ w_E, w_F	Weighting factors for CAIDI, SAIDI, EENS, and SAIFI.
$\alpha_{n,i}$	Parameter relating node n to feeder section i, which is equal to -1 if load node n is the sending node of feeder section i, 1 if load node n is the receiving node of feeder section i, and 0 otherwise.
λ_i	Failure rate of feeder section i.
σ	Total network demand per consumer.
$\chi_{k,m}$	Binary parameter, which is equal to 1 if feeder section k is in path m, being 0 otherwise.

Variables

AENS	Average energy not served.
ASAI	Average service availability index.
ASUI	Average service unavailability index.
CAIDI	Customer average interruption duration index.

*Corresponding author
Email address: mohammad.jooshaki@gtk.fi (Mohammad Jooshaki)

$EENS$	Expected energy not served.
f_i^o, f_i^p	Variables that are equal to the total demand downstream of feeder section i if the feeder section is in service and its fictitious flow direction is opposite (o) or equal (p) to the predetermined direction, being 0 otherwise.
g_i^o, g_i^p	Variables that are equal to the total DG capacity connected to the nodes downstream of feeder section i if the feeder section is in service and its fictitious flow direction is opposite (o) or equal (p) to the predetermined direction, being 0 otherwise.
g_n	Total demand served by the substation connected to node n.
g_n^C	Power injected by the substation located at node n in the fictitious system used to model CAIDI.
g_n^{DG}	Total DG capacity connected to the feeders served by the substation located at node n.
g_n^N	Total number of customers served by the substation located at node n.
n_i^o, n_i^p	Variables that are equal to the total number of customers connected to the nodes downstream of feeder section i if the feeder section is in service and its fictitious flow direction is opposite (o) or equal (p) to the predetermined direction, being 0 otherwise.
n_i^r, n_i^s	Total numbers of customers interrupted during the repair and switching processes following the failure of feeder section i.
P_i^r, P_i^s	Total demands curtailed during the repair and switching processes following the failure of feeder section i.
$SAIDI$	System average interruption duration index.
$SAIFI$	System average interruption frequency index.
y_i^o, y_i^p	Binary utilization variables for feeder section i.
$z_{i,j}$	Binary-valued continuous variable, which is equal to 1 if feeder section i is in a feeder whose first branch is feeder section j and the switch of feeder section i is closed, being 0 otherwise.
$\beta_i^o, \beta_i^p, \beta_i^s$	Auxiliary variables used to model CAIDI.
δ_n	Average annual duration of customer outages at node n.

1. Introduction

The provision of service reliability typically accounts for almost half of the total distribution system costs [1], while even more investments are expected to be required to achieve the same reliability level in the future grids [2]. Considering such a notable share, reliability plays a key role in minimizing planning and operating costs of electricity distribution networks. In order to quantify the reliability of distribution grids, several indices are used. System average interruption duration index (SAIDI), system average interruption frequency index (SAIFI), customer average interruption duration index (CAIDI), average service availability index (ASAI), and expected energy not served (EENS) are among the most widely used reliability indices by the power industry [1–5]. Considering that each index is related to a specific aspect of service reliability, a set of different indices is leveraged in practice to characterize network reliability. A typical combination includes SAIFI, SAIDI, and CAIDI [2], where SAIFI is used to track the number of interruptions, whereas SAIDI and CAIDI measure the duration of customer interruptions from two different perspectives. Unlike SAIDI, which indicates the average duration of service disruption over all consumers of a utility, CAIDI focuses on customer-interruption quantification by representing the average duration of an interruption. Thus, compared to SAIDI, CAIDI may be more appealing in several applications due to its per-event nature, which more intuitively reflects the efforts made to reduce the restoration time following a network contingency [6]. Accordingly, CAIDI is of utmost practical importance and customarily considered by distribution companies and regulatory authorities [1, 2, 4, 7].

Notwithstanding the concrete theoretical basis of distribution reliability and the extensive research conducted, incorporating reliability in distribution system optimization problems without resorting to approximate methods is still a major challenge when the optimal network topology is an outcome of the model. Note that expressing the mathematical relationship between standard reliability indices and network topology is nontrivial when such a topology is not specified a priori. Distribution system expansion planning and network reconfiguration are among such problems. Taking distribution network reconfiguration as an example, the objective is to find the optimal radial topology to often minimize operational costs or improve system reliability [8]. Within this context, the application of the traditional failure modes and effects analysis (FMEA) [1], upon which the majority of available distribution reliability models have been developed, is highly problematic. This is because the consequences of network contingencies depend on the operational topology of the grid. For instance, a load node can be affected by the failure of a feeder section in one operational topology, whereas this may not be the case for other topologies.

In the existing literature, efficient methods have been proposed for evaluating the reliability of distribution networks with definite topologies [9–13]. In other words, such techniques are applicable only if the states of all the network switches are known a priori. Under this assumption, the effect of each failure mode on the consumers can be assessed based on the network connectivity. In addition, since the location of tie lines is given, the impact of post-fault remedial actions is relatively straightforward to model. Thus, built upon the assumption of a known network topology, the state-of-the-art topology-parameterized reliability models are capable of quantifying the reliability of distribution grids with a high level of ac-

curacy. However, such models cannot be applied in the cases where the network topology at the optimal solution is unidentified. Moreover, for practical mesh-designed distribution networks, an exhaustive search among the enormous number of possible operational topologies is also impractical. Attempting to address this issue, heuristic [14, 15] and meta-heuristic [16–18] optimization techniques have been leveraged to account for reliability in distribution network studies. Unfortunately, such algorithms neither guarantee achieving optimality nor provide a measure of the distance to the global optimum.

The idea of explicitly characterizing the topological dependence of reliability for a distribution network can be traced back to [19], where a mathematical-programming-based model is presented for network reconfiguration to minimize energy loss and enhance the network reliability. Nonetheless, the reliability assessment technique developed in [19] only accounts for failures of the branches upstream of every node, whereas the switching interruptions caused by the faults on the downstream feeder sections are neglected. The modeling capability of topology-variable-based distribution reliability assessment has been extended in [20], where linear expressions are devised to model distribution reliability indices. The reliability assessment technique presented in [20] has been successfully applied to distribution system expansion planning [21] and microgrid design disregarding switching interruptions [22]. Yet, embedding the formulation proposed in [20] into an optimization problem adds an excessive number of decision variables and constraints to the resulting model, which may drastically increase the computational burden. This shortcoming has been addressed in [23] through an efficient algebraic model for distribution reliability evaluation. Nevertheless, the reliability models in [20–23] are unsuitable to represent the system-wide effect of distributed generation (DG) units on reliability as they are particularly tailored to passive distribution networks, being only able to consider DG in the form of nonnegative nodal net demands. In [24, 25], contingency-constrained formulations have been presented for optimization-based reliability assessment of distribution systems considering post-fault network reconfiguration and the placement of circuit breakers and switches. The reliability models presented in [24] have been recently adopted in [26, 27] for the expansion planning of passive distribution networks. Unfortunately, the formulations derived in [24, 25] require the integration of operational constraints for all failure states considered for contingency analysis, thereby giving rise to dimensionality issues for real-size networks. Moreover, the models presented in [20–27] rely on node-level reliability parameters, i.e., the average failure rate and the average annual outage time of each load node, to eventually characterize system-level metrics, e.g., SAIFI and SAIDI. This aspect poses serious challenges for 1) the extension of those formulations to active distribution networks, which requires considering the complex and topology-dependent impact of DG on the restoration times of load nodes under various failure scenarios, and 2) the quantification of customer interruptions through the practical index CAIDI, which is related to load-node indices and to SAIDI and SAIFI in a nonlinear and nonconvex fashion.

An alternative technique has been proposed in [28] for the straightforward modeling of system-level reliability indices. The model presented in [28] has been extended in [29] to capture the system-wide impact of DG units on the reliability metrics. Nevertheless, similar to [19, 22], the reliability evaluation methods in [28, 29] both feature oversimplifications resulting from neglecting switching interruptions. Aiming to overcome this issue, in [30], a promising approach is proposed for the straightforward calculation of system-oriented reliability metrics while also considering switching interruptions. Built upon the model formulated in [30], an equivalent variant with fewer constraints is presented in [31] to enhance the computational performance. Recently, the reliability evaluation technique introduced in [30] has been further developed in [32] to devise a model for reliability-constrained multistage distribution network expansion planning. However, in [30–32], the reliability assessment is restricted to passive distribution networks and a reduced set of linear and non-customer-oriented metrics, namely SAIDI, SAIFI, and EENS. Hence, both DG and CAIDI are disregarded therein.

Within the context of distribution reliability assessment based on the explicit formulation of the inherent dependence on network topology [19–32], the thrust of this paper is to fill an important gap of the relevant literature by presenting a novel mixed-integer linear programming (MILP) model jointly considering dispatchable DG units, switching interruptions, and a complete set of practical reliability metrics including the nonlinear and nonconvex customer-oriented CAIDI. Note that MILP provides a sound mathematical framework with well-known properties in terms of convergence and solution quality. Moreover, the use of standard commercial software is allowed. The main differences between this paper and the state of the art are summarized in Table 1.

The main contributions of this paper are thus twofold:

1. A new MILP-based, system-oriented model is presented for the reliability assessment of active distribution networks with unknown topology. This model represents a substantial departure from the closely related literature [19–32] as both dispatchable DG units and switching interruptions are jointly considered.
2. The intrinsic nonlinearity and nonconvexity of CAIDI are equivalently characterized by an original MILP-based formulation. Thus, in the absence of explicit topology-dependent formulations in state-of-the-art works [19–32], the use of exact solution techniques is enabled, for the first time, to handle this practical customer-oriented index.

Table 1: Proposed Approach versus the State of the Art

	[9, 14, 16–18]	[10, 11, 13, 15]	[12]	[19, 22]	[20, 21, 23–27]	[28]	[29]	[30–32]	Proposed approach
Explicit formulation of topology dependence	✗	✗	✗	✓	✓	✓	✓	✓	✓
System-wide impact of DG	✗	✓	✓	✗	✗	✗	✓	✗	✓
Switching interruptions	✓	✓	✗	✗	✓	✗	✗	✓	✓
Linear model for CAIDI	✗	✗	✗	✗	✗	✗	✗	✗	✓
Direct calculation of system-level reliability indices	✗	✗	✗	✗	✗	✓	✓	✓	✓

The significance of the contributions reported in this paper is twofold:

1. To the best of our knowledge, there is no current literature contribution on distribution reliability assessment under unknown network topology describing the joint consideration of dispatchable distributed generation and switching interruptions. Thus, the proposed reliability assessment is not limited to considering either passive networks or the effects of failures occurring in the shortest upstream path between each load node and the corresponding substation. Moreover, for the first time, the practical nonlinear and nonconvex CAIDI is equivalently cast using mixed-integer linear programming.
2. Devising a mixed-integer linear programming formulation paves the way for the use of the standard branch-and-cut algorithm, which guarantees finite convergence to optimality while providing a measure of the distance to the global optimum along the solution process. Additionally, efficient off-the-shelf software is readily available, which is advantageous for practical implementation purposes.

Therefore, a more accurate assessment of reliability is provided without relying on heuristics or simulation, which is particularly relevant for industry practice.

The remainder of this paper is organized as follows. Section 2 presents the modeling framework. Section 3 describes the novel expressions for reliability assessment. Section 4 is devoted to the application of the proposed model to the reliability-constrained optimal network reconfiguration problem of meshed grids. In Section 5, numerical results from several case studies are discussed. Finally, relevant conclusions are drawn in Section 6.

2. Modeling Framework

Under the framework of explicit formulations for the topological dependence of reliability assessment, we adopt the modeling aspects commonly considered in [20, 21, 23, 28–32], which are consistent with the depth of analysis required for the target optimization models. Accordingly, the sequence of events associated with the failure of a feeder section comprises four states, as shown for the illustrative example depicted in Fig. 1:

State 1: A fault occurs on a feeder section, e.g., feeder section $l2$ in Fig. 1.

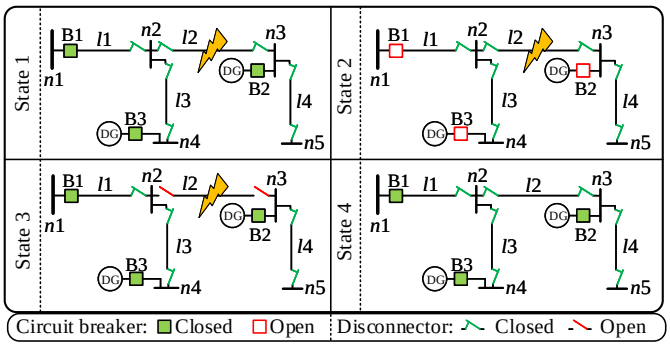

Figure 1: Illustrative radial network – System states following a feeder section failure.

State 2: All circuit breakers trip to interrupt the fault current.

State 3: After the switching time, the faulty feeder section is isolated by opening its disconnecting switches, and the circuit breakers are closed to reenergize the healthy sections of the network.

State 4: After repairing or replacing the affected conductors in the faulty feeder section, the corresponding disconnectors are closed, and the network returns to its normal operation.

Thus, when a fault occurs on a feeder section, the whole demand of the corresponding feeder is interrupted during the time required for the transition from State 1 to State 3, known as switching time. During the transition from State 3 to State 4, hereinafter referred to as repair time, part of the demand downstream of the faulty feeder section might experience power outage due to the shortage of DG capacity in the islanded section, e.g., nodes $n3$ and $n5$ in State 3 for Fig. 1. Note that the time required for fault location is included in the aforementioned switching and repair times.

The calculation of the corresponding reliability indices requires the identification of the frequency and duration of interruptions as well as the amount of power and the number of customers interrupted due to the failure of each feeder section. This information can be readily obtained for distribution networks with known radial topologies, since the consequences of a feeder section failure can be determined based on the network configuration. For instance, assuming that the overall capacity of DG units is dispatchable and sufficiently large to supply the whole demand in the islanded zones during contingencies, the effects of feeder section failures for the network depicted in

Table 2: Illustrative Radial Network – Effects of Feeder Section Failures on Load Nodes

Faulty feeder section	Frequency				Duration			
	$n2$	$n3$	$n4$	$n5$	$n2$	$n3$	$n4$	$n5$
$l1$	λ_1	λ_1	λ_1	λ_1	$\lambda_1 s_1$	$\lambda_1 s_1$	$\lambda_1 s_1$	$\lambda_1 s_1$
$l2$	λ_2	λ_2	λ_2	λ_2	$\lambda_2 s_2$	$\lambda_2 s_2$	$\lambda_2 s_2$	$\lambda_2 s_2$
$l3$	λ_3	λ_3	λ_3	λ_3	$\lambda_3 s_3$	$\lambda_3 s_3$	$\lambda_3 s_3$	$\lambda_3 s_3$
$l4$	λ_4	λ_4	λ_4	λ_4	$\lambda_4 s_4$	$\lambda_4 s_4$	$\lambda_4 s_4$	$\lambda_4 (s_4 + r_4)$

Minimum expected durations assuming DG support under contingency

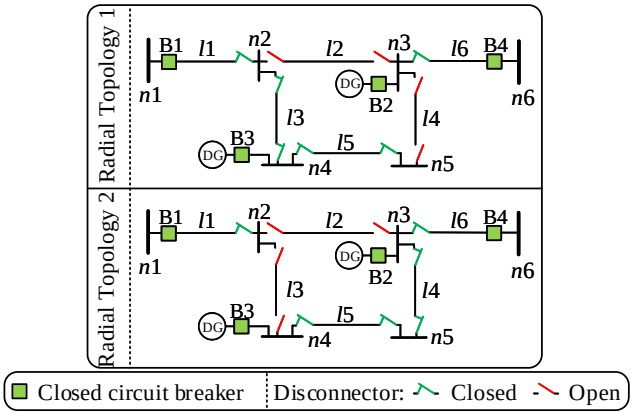

Figure 2: Illustrative mesh-designed network – Examples of radial operational topologies.

Fig. 1 are provided in Table 2. As per this table, it can be inferred that, as an example, the failure of feeder section $l1$ causes the outage of all the demands connected to load nodes $n2$–$n5$ for the switching time s_1. On the other hand, if we disregard the contingency support from DG units, repair times, r_i, should be added to the switching times, s_i, in the shaded cells of this table, which may lead to significantly longer interruption durations. Thus, DG units can reduce the duration of interruptions, thereby improving reliability. In practice, active distribution networks typically operate somewhere between these two extreme cases, i.e., DG units can only serve a portion of the demand connected to the isolated nodes. Thus, in our proposed model, we consider the available capacity of dispatchable DG for contingency support. It goes without saying that DG has no impact on the frequency of interruptions unless the network is highly automated such that the switching times are shorter than the minimum threshold – typically, 3 or 5 minutes – considered in the definition of distribution reliability metrics.

Unfortunately, albeit radially operated, distribution systems typically have a meshed design [1, 30]. Hence, reliability depends on the radial operational topology. Let us consider the simple mesh-designed distribution network depicted in Fig. 2 as an example. Assuming that 1) the capacities of feeder sections are large enough, and 2) the voltage drops are negligible, this network can be operated under ten different radial configurations, each resulting from switching off a pair of feeder sections from the set $\{(l1, l2), (l1, l3), (l1, l4), (l1, l5), (l2, l3), (l2, l4), (l2, l5), (l2, l6), (l3, l6), (l4, l6)\}$. Note that a configuration is considered radial if only one path exists from any load node to one of the substation nodes.

Fig. 2 is also useful to illustrate how the consequence of a feeder section failure drastically varies depending on the radial topology used for operation. For instance, let us examine the effect of a fault on feeder section $l6$ for the two topologies depicted in Fig. 2. In the first topology, such a failure results in the tripping of circuit breakers B2 and B4, and, thus, power interruption for the customers connected to node $n3$. On the other hand, in the second topology, the outage of feeder section $l6$ also affects nodes $n4$ and $n5$ due to the operation of circuit breakers B2–B4.

The main goal of this paper is the development of an explicit formulation characterizing the topological dependence of standard reliability indices including the practical, albeit nonlinear and nonconvex, CAIDI, while considering the effect of DG and switching interruptions, thereby overcoming the limitations of state-of-the-art approaches [19–32].

3. Proposed Reliability Assessment Model

In reliability-constrained optimization models, the system cost, including reliability-related or interruption cost terms, is minimized subject to a set of constrained functions representing system operation and/or planning as well as reliability metrics. In this section, reliability indices for active distribution networks are modeled by mixed-integer linear expressions without using extra binary variables, which may be advantageous from a computational perspective.

3.1. Expected Energy Not Served

EENS is typically cast as [7]:

$$EENS = \sum\nolimits_{n \in \Omega^D} \delta_n D_n. \tag{1}$$

However, within the context of optimization models for distribution network operation and planning, modeling nodal outage durations δ_n is quite challenging, especially in the presence of DG units. Alternatively, EENS can be equivalently formulated in terms of the load curtailment associated with the outages of feeder sections [30]:

$$EENS = \sum\nolimits_{i \in \Pi} \lambda_i \left(s_i P_i^s + r_i P_i^r \right). \tag{2}$$

A novel mixed-integer linear formulation for P_i^s and P_i^r is presented next.

3.1.1. Model for P_i^s

As shown in Fig. 1 for the illustrative five-node example, when a fault occurs on a feeder section i, the supply of the total demand connected to the feeder to which feeder

section i belongs is interrupted during the switching time. Thus, P_i^s is equal to the total demand of the feeder that includes feeder section i. In order to model P_i^s, $\forall i \in \Pi$, we propose the application of Kirchhoff's current law (KCL) to a fictitious lossless network with the same topology as the network under consideration in which all DG units are dropped. KCL for this fictitious network is modeled in (3)–(9):

$$\sum\nolimits_{i\in\Pi} \alpha_{n,i}\,(f_i^p - f_i^o) - D_n = 0; \forall n \in \Omega^D \tag{3}$$

$$\sum\nolimits_{i\in\Pi} \alpha_{n,i}\,(f_i^p - f_i^o) + g_n = 0; \forall n \in \Omega^S \tag{4}$$

$$0 \le f_i^p \le M y_i^p; \forall i \in \Pi \tag{5}$$

$$0 \le f_i^o \le M y_i^o; \forall i \in \Pi \tag{6}$$

$$y_i^o, y_i^p \in \{0,1\}; \forall i \in \Pi \tag{7}$$

$$y_i^p + y_i^o \le 1; \forall i \in \Pi \tag{8}$$

$$\sum_{i\in\Pi|\alpha_{n,i}=-1} y_i^o + \sum_{i\in\Pi|\alpha_{n,i}=1} y_i^p = 1; \forall n \in \Omega^D. \tag{9}$$

In this model, for every feeder section i, a predetermined flow direction is arbitrarily selected through parameters $\alpha_{n,i}$, whereas two binary variables, y_i^p and y_i^o, are used to represent the actual flow direction. In case feeder section i is in service and its flow direction is consistent with the predetermined direction, y_i^p becomes 1 and y_i^o is equal to 0. On the other hand, if the flow direction is against the predetermined direction, y_i^p is equal to 0 and y_i^o becomes 1. Otherwise, when the feeder section is switched off, both y_i^p and y_i^o are equal to 0.

Expressions (3) and (4) are the power balance at fictitious load and substation nodes, respectively. Constraints (5) and (6) set the bounds for fictitious flow variables f_i^p and f_i^o based on the corresponding feeder-section state represented by binary utilization variables y_i^p and y_i^o. Expressions (7) model the binary nature of y_i^p and y_i^o. As per (8), only one of the two binary variables y_i^p and y_i^o can take a non-zero value for each feeder section. Radial operation is imposed in (9), whereby the number of supplying feeder sections per load node is set to 1 [21]. In other words, for a radial topology, from all feeder sections connected to a given load node n, there must be only one with a flow direction toward node n.

Considering the radial operation of the network, expressions (3)–(8) set the absolute value of the fictitious power flow of each feeder section i, i.e., $f_i^p + f_i^o$, equal to the total demand downstream of that feeder section [28–32]. Thus, the total demand of a feeder is equal to the fictitious flow of its first feeder section, i.e., the branch located at the sending extreme of the feeder. In other words, for a feeder section i directly connected to a substation node, either f_i^p or f_i^o is equal to the total demand connected to the corresponding feeder.

It should be noted that the first branch of the feeder to which feeder section i belongs depends on the radial topology of the network modeled by utilization variables y_i^p and y_i^o. This topology-related aspect is formulated as follows:

$$\sum\nolimits_{j\in\Pi^S} z_{i,j} = y_i^p + y_i^o; \forall i \in \Pi \setminus \Pi^S \tag{10}$$

$$z_{i,j} \ge 1 + \sum\nolimits_{k\in\Pi} \chi_{k,m}\,(y_k^p + y_k^o - 1)\,; \quad \forall i \in \Pi \setminus \Pi^S, \forall j \in \Pi^S, \forall m \in \Psi_{i,j} \tag{11}$$

$$z_{i,j} \ge 0; \forall i \in \Pi \setminus \Pi^S, \forall j \in \Pi^S \tag{12}$$

where $z_{i,j}$ is a binary-valued continuous variable, which is equal to 1 if feeder section j is the first feeder section corresponding to feeder section i, being 0 otherwise.

According to (10) and (12), if feeder section i is not in service, i.e., $y_i^p + y_i^o$ is equal to 0, then $z_{i,j} = 0$, $\forall j \in \Pi^S$, as the notion of first feeder section does not apply. Conversely, if feeder section i is in service, i.e., $y_i^p + y_i^o$ is equal to 1, then $z_{i,j}$ must be greater than 0 for some feeder section j connected to a substation, as per (10) and (12). More specifically, expressions (10)–(12) ensure that the first feeder section j of feeder section i is flagged by the corresponding $z_{i,j}$ being equal to 1 and all other $z_{i,j}$ being equal to 0. Note that, in (11), the lower bound for $z_{i,j}$ is set to 1 in case there is a path between feeder sections i and j in which all feeder sections are in service. Otherwise, the right-hand side of (11) becomes an integer less than 1, thereby giving rise to a lower bound that is less tight than that set in (12). Bearing in mind the radial operation of the network imposed by (9), only one such path exists between feeder section i and all possible first feeder sections j. Thus, for a given feeder section i in service, the corresponding expression (10) only holds true if all $z_{i,j}$ are equal to their tightest lower bounds, i.e., $z_{i,j} = 1$ for a single index j and 0 for the others, as desired.

Expressions (10)–(12) are exemplified through their application to feeder section $l3$ in the mesh-designed network shown in Fig. 2, i.e., $i = l3$. Feeder sections $l1$ and $l6$ are directly connected to substation nodes, thus, $\Pi^S = \{l1, l6\}$. Note also that there are three paths connecting feeder section $l3$ to a substation, namely $l1$-$l3$, $l2$-$l3$-$l6$, and $l3$-$l4$-$l5$-$l6$, which are indexed by $m1$–$m3$, respectively. Hence, $\Psi_{l3,l1} = \{m1\}$ and $\Psi_{l3,l6} = \{m2, m3\}$. Besides:

$$\chi_{l1,m1} = \chi_{l3,m1} = 1,\ \chi_{l2,m1} = \chi_{l4,m1} = \chi_{l5,m1} = \chi_{l6,m1} = 0;$$
$$\chi_{l2,m2} = \chi_{l3,m2} = \chi_{l6,m2} = 1,\ \chi_{l1,m2} = \chi_{l4,m2} = \chi_{l5,m2} = 0;$$
$$\chi_{l3,m3} = \chi_{l4,m3} = \chi_{l5,m3} = \chi_{l6,m3} = 1,\ \chi_{l1,m3} = \chi_{l2,m3} = 0.$$

For illustration purposes, let us consider Radial Topology 1 depicted in Fig. 2, for which the binary utilization variables meet the following expressions:

$$(y^p_{l1} + y^o_{l1}) = (y^p_{l3} + y^o_{l3}) = (y^p_{l5} + y^o_{l5}) = (y^p_{l6} + y^o_{l6}) = 1;$$
$$(y^p_{l2} + y^o_{l2}) = (y^p_{l4} + y^o_{l4}) = 0.$$

Thus, based on (10)–(12), we get:

$$z_{l3,l1} + z_{l3,l6} = y^p_{l3} + y^o_{l3} = 1;$$

$$z_{l3,l1} \geq 1 + (y^p_{l1} + y^o_{l1} - 1) + (y^p_{l3} + y^o_{l3} - 1) = 1;$$

$$z_{l3,l6} \geq 1 + (y^p_{l2} + y^o_{l2} - 1) + (y^p_{l3} + y^o_{l3} - 1) + (y^p_{l6} + y^o_{l6} - 1) = 0;$$

$$z_{l3,l6} \geq 1 + (y^p_{l3} + y^o_{l3} - 1) + (y^p_{l4} + y^o_{l4} - 1) + (y^p_{l5} + y^o_{l5} - 1) + (y^p_{l6} + y^o_{l6} - 1) = 0;$$

$$z_{l3,l1} \geq 0;$$

$$z_{l3,l6} \geq 0.$$

These expressions hold true only if $z_{l3,l1} = 1$ and $z_{l3,l6} = 0$, as desired.

Using $z_{i,j}$, the total demand of the feeder corresponding to each feeder section P^s_i can be readily expressed as below:

$$P^s_i = \sum\nolimits_{j \in \Pi^S} z_{i,j} (f^p_j + f^o_j); \forall i \in \Pi \setminus \Pi^S \tag{13}$$

$$P^s_i = f^p_i + f^o_i; \forall i \in \Pi^S. \tag{14}$$

Expressions (13) are nonlinear due to the bilinear terms $z_{i,j} f^p_j$ and $z_{i,j} f^o_j$. Such nonlinearities can be sorted out by replacing (13) with:

$$P^s_i \geq (f^p_j + f^o_j) - M(1 - z_{i,j}); \forall i \in \Pi \setminus \Pi^S, \forall j \in \Pi^S \tag{15}$$

$$P^s_i \geq 0; \forall i \in \Pi \setminus \Pi^S. \tag{16}$$

Note that the reliability-constrained optimization models for which this formulation is intended are driven by the minimization of an objective function that is strictly increasing with respect to EENS, and, hence, P^s_i, since the higher the EENS, the greater the interruption cost. Thus, P^s_i is equal to its lower bound at the optimal solution. Expressions (15) and (16) set the lower bound for P^s_i to the desired value, which is $f^p_j + f^o_j$ if $z_{i,j}$ is equal to 1, and 0 otherwise.

3.1.2. Model for P^r_i

Based on the remarks explained in Section 2 and the strictly increasing behavior of the objective function of the target model with respect to P^r_i, the demand interrupted during the repair of a faulty feeder section i, i.e., P^r_i, is modeled by the following bounding constraints:

$$P^r_i \geq (f^p_i + f^o_i) - (g^p_i + g^o_i); \forall i \in \Pi \tag{17}$$

$$P^r_i \geq 0; \forall i \in \Pi. \tag{18}$$

For every feeder section i, the right-hand side of (17) models the difference between the total downstream demand, represented by the sum of the above-described f^p_i and f^o_i, and the total downstream DG capacity, expressed by the sum of additional variables g^p_i and g^o_i that are associated with the application of KCL to another fictitious network as described below. If the total DG capacity downstream of feeder section i is not sufficient to supply the total demand in the zone downstream of that feeder section, the extra demand curtailed during the repair of such a feeder section is modeled by the right-hand side of (17), which becomes a positive value. Thus, the optimization process sets P^r_i equal to the lower bound resulting from (17), which is tighter than the nonnegativity imposed in (18). Conversely, if the total DG capacity in the islanded zone downstream of feeder section i is greater than its total demand, the right-hand side of (17) becomes negative, and, hence, the lower bound for P^r_i is set to 0 by (18).

In order to model g^p_i and g^o_i, KCL equations are applied to a lossless fictitious network with the same topology as the original distribution network, in which the fictitious nodal demands are set equal to the connected DG capacities, using (19)–(23):

$$\sum\nolimits_{i \in \Pi} \alpha_{n,i} (g^p_i - g^o_i) - G_n = 0; \forall n \in \Omega^{DG} \tag{19}$$

$$\sum\nolimits_{i \in \Pi} \alpha_{n,i} (g^p_i - g^o_i) = 0; \forall n \in \Omega^{D} \setminus \Omega^{DG} \tag{20}$$

$$\sum\nolimits_{i \in \Pi} \alpha_{n,i} (g^p_i - g^o_i) + g^{DG}_n = 0; \forall n \in \Omega^{S} \tag{21}$$

$$0 \leq g^p_i \leq M y^p_i; \forall i \in \Pi \tag{22}$$

$$0 \leq g^o_i \leq M y^o_i; \forall i \in \Pi. \tag{23}$$

Expressions (19)–(21) represent the power balance at DG nodes, load nodes without DG, and substation nodes, respectively. Structurally identical to (5) and (6), constraints (22) and (23) bound g^p_i and g^o_i, respectively.

It should be noted that the combined use of 1) the concepts denoted by P^r_i and P^s_i, 2) KCL for a fictitious network, and 3) two binary variables for branch operation represents the main novelty of the above model (3)–(23) with respect to available explicit formulations for EENS [19–32].

3.2. System Average Interruption Duration Index

SAIDI is customarily cast as (24) [7]:

$$SAIDI = \frac{\sum_{n\in\Omega^D} \delta_n N_n}{\sum_{n\in\Omega^D} N_n}. \tag{24}$$

In order to avoid modeling δ_n, the traditional SAIDI expression (24) is equivalently reformulated as (25), which is analogous to (2) [30]:

$$SAIDI = \frac{\sum_{i\in\Pi} \lambda_i (s_i n_i^s + r_i n_i^r)}{\sum_{n\in\Omega^D} N_n}. \tag{25}$$

Based on the explanations for the EENS model, the number of customers disconnected during the switching process due to the failure of feeder section i, i.e., n_i^s, is equal to the total number of customers connected to the corresponding feeder. Thus, following the same procedure employed for modeling P_i^s, expressions (26)–(29) are used to identify the total number of customers connected to the nodes downstream of every feeder section:

$$\sum\nolimits_{i\in\Pi} \alpha_{n,i} \left(n_i^p - n_i^o\right) - N_n = 0; \forall n \in \Omega^D \tag{26}$$

$$\sum\nolimits_{i\in\Pi} \alpha_{n,i} \left(n_i^p - n_i^o\right) + g_n^N = 0; \forall n \in \Omega^S \tag{27}$$

$$0 \leq n_i^p \leq M y_i^p; \forall i \in \Pi \tag{28}$$

$$0 \leq n_i^o \leq M y_i^o; \forall i \in \Pi. \tag{29}$$

Expressions (26)–(29) model KCL for a fictitious network whose demand at each node n is set to the total number of customers connected to that node, i.e., N_n. The power balance at load and substation nodes of such a fictitious network is modeled by (26) and (27), respectively. Constraints (28) and (29) respectively set the bounds for auxiliary variables n_i^p and n_i^o.

Using n_i^p and n_i^o, n_i^s is cast by (30) and (31), which are structurally identical to (13) and (14):

$$n_i^s = \sum\nolimits_{j\in\Pi^S} z_{i,j} (n_j^p + n_j^o); \forall i \in \Pi \setminus \Pi^S \tag{30}$$

$$n_i^s = n_i^p + n_i^o; \forall i \in \Pi^S. \tag{31}$$

As done for (13), expressions (30) can be equivalently modeled in a linear form using (32) and (33):

$$n_i^s \geq (n_j^p + n_j^o) - M(1 - z_{i,j}); \forall i \in \Pi \setminus \Pi^S, \forall j \in \Pi^S \tag{32}$$

$$n_i^s \geq 0; \forall i \in \Pi \setminus \Pi^S. \tag{33}$$

The number of customers that remain interrupted during the repair of the faulty feeder section i, n_i^r, is modeled by (34) and (35):

$$n_i^r \geq (n_i^p + n_i^o) - \frac{(g_i^p + g_i^o)}{\sigma}; \forall i \in \Pi \tag{34}$$

$$n_i^r \geq 0; \forall i \in \Pi. \tag{35}$$

Considering the fact that a higher SAIDI yields a greater interruption cost, the system cost minimized in reliability-constrained optimization models is strictly increasing with respect to n_i^r. Thus, n_i^r is set to its tightest lower bound at the optimal solution. When the total DG capacity in the zone downstream of feeder section i is insufficient to supply its whole demand, the right-hand side of (34) takes a positive value determining the estimated number of curtailed customers. Otherwise, the right-hand side of (34) is negative and the lower bound for n_i^r is set to 0 by (35).

It is worth emphasizing that expressions (26)–(35) constitute a distinctive feature over the state-of-the-art approaches [19–32].

3.3. System Average Interruption Frequency Index

SAIFI is defined as the total number of customer interruptions per the total number of customers connected to the distribution network [7]. Since the failure of a feeder section results in the interruption of all the customers connected to the corresponding feeder, SAIFI can be readily cast as (36):

$$SAIFI = \frac{\sum_{i\in\Pi} \lambda_i n_i^s}{\sum_{n\in\Omega^D} N_n}. \tag{36}$$

3.4. Customer Average Interruption Duration Index

CAIDI is typically defined by (37) [4]:

$$CAIDI = \frac{SAIDI}{SAIFI}. \tag{37}$$

As both $SAIDI$ and $SAIFI$ are decision variables when explicitly formulating the topological dependence of reliability assessment, expression (37) is nonlinear and nonconvex, and is thus typically neglected in the relevant literature [19–32]. Here, as a major novelty over [19–32], we present an equivalent reformulation of (37) relying on mixed-integer linear programming. To that end, using (25) and (36) in (37) yields:

$$CAIDI = \frac{\sum_{i\in\Pi} \lambda_i (s_i n_i^s + r_i n_i^r)}{\sum_{i\in\Pi} \lambda_i n_i^s}. \tag{38}$$

Unfortunately, expression (38) is still nonlinear and nonconvex. In order to devise a linear model for CAIDI, we introduce auxiliary variables β_i^s, such that:

$$\beta_i^s = n_i^s CAIDI; \forall i \in \Pi. \tag{39}$$

Using (39), expression (38) becomes:

$$\sum\nolimits_{i\in\Pi} \lambda_i \beta_i^s = \sum\nolimits_{i\in\Pi} \lambda_i (s_i n_i^s + r_i n_i^r). \tag{40}$$

Note that expression (40) is linear, whereas the nonlinearity of (39) can be sorted out based on the relationship

between β_i^s and n_i^s and leveraging the process described in Section 3.2 to model n_i^s. Thus, from (30) and (31), expressions (39) can be rewritten as (41) and (42):

$$\begin{aligned}\beta_i^s &= CAIDI \sum\nolimits_{j\in\Pi^S} z_{i,j}(n_j^p + n_j^o) \\ &= \sum\nolimits_{j\in\Pi^S} z_{i,j}(n_j^p\, CAIDI + n_j^o\, CAIDI); \forall i \in \Pi\setminus\Pi^S \end{aligned} \quad (41)$$

$$\beta_i^s = n_i^p\, CAIDI + n_i^o\, CAIDI; \forall i \in \Pi^S. \quad (42)$$

Similar to β_i^s, nonlinear terms $n_i^p\, CAIDI$ and $n_i^o\, CAIDI$ can be respectively replaced with additional auxiliary variables β_i^p and β_i^o, which allows transforming (41) and (42) into:

$$\beta_i^s = \sum\nolimits_{j\in\Pi^S} z_{i,j}(\beta_j^p + \beta_j^o); \forall i \in \Pi \setminus \Pi^S \quad (43)$$

$$\beta_i^s = \beta_i^p + \beta_i^o; \forall i \in \Pi^S. \quad (44)$$

Moreover, bearing in mind that β_i^p and β_i^o are respectively equal to n_i^p and n_i^o times $CAIDI$, KCL-based expressions (26)–(29) modeling n_i^p and n_i^o can be adapted to characterize β_i^p and β_i^o as follows:

$$\sum\nolimits_{i\in\Pi} \alpha_{n,i}\,(\beta_i^p - \beta_i^o) - N_n\, CAIDI = 0; \forall n \in \Omega^D \quad (45)$$

$$\sum\nolimits_{i\in\Pi} \alpha_{n,i}\,(\beta_i^p - \beta_i^o) + g_n^C = 0; \forall n \in \Omega^S \quad (46)$$

$$0 \le \beta_i^p \le M y_i^p; \forall i \in \Pi \quad (47)$$

$$0 \le \beta_i^o \le M y_i^o; \forall i \in \Pi \quad (48)$$

where the loading condition of the fictitious network corresponds to that of (26)–(29) times $CAIDI$.

The nonlinearity in (43), i.e., the multiplication term $z_{i,j}(\beta_j^p + \beta_j^o)$, can also be linearized as (49) and (50):

$$\begin{aligned}-M(1 - z_{i,j}) \le \beta_i^s - (\beta_j^p + \beta_j^o) \le M(1 - z_{i,j}); \\ \forall i \in \Pi \setminus \Pi^S, \forall j \in \Pi^S \end{aligned} \quad (49)$$

$$0 \le \beta_i^s \le M \sum\nolimits_{j\in\Pi^S} z_{i,j}; \forall i \in \Pi \setminus \Pi^S. \quad (50)$$

Note that since the system cost bears no direct relation to β_i^s, i.e., monotonically increasing or decreasing, we tightly set both the lower and upper bounds for β_i^s in (49) and (50), in contrast to the linearization of (13) in (15) and (16).

3.5. Average Service Availability (Unavailability) Index

ASAI is customarily modeled as (51) [7]:

$$ASAI = 1 - \frac{\sum_{n\in\Omega^D} \delta_n N_n}{\sum_{n\in\Omega^D} 8760 N_n}. \quad (51)$$

According to (24), ASAI can also be expressed as:

$$ASAI = 1 - \frac{SAIDI}{8760}. \quad (52)$$

Analogously, ASUI can be readily expressed as:

$$ASUI = 1 - ASAI = \frac{SAIDI}{8760}. \quad (53)$$

Thus, both ASAI and ASUI can be represented by the proposed model for SAIDI described in Section 3.2.

3.6. Average Energy Not Supplied

AENS is defined as the total annual energy curtailed per the total number of customers served by the distribution network [7]:

$$AENS = \frac{EENS}{\sum_{n\in\Omega^D} N_n}. \quad (54)$$

Thus, using the model for EENS proposed in Section 3.1, AENS can be readily cast.

4. Application

Since the reliability evaluation model devised in the previous section is based on mixed-integer linear programming, it can be readily incorporated into various standard mathematical-programming-based models associated with the operation and planning of distribution networks. In this section, the proposed reliability assessment approach is employed in a distribution system reconfiguration problem [8]. To place the focus on network reliability, we consider that the determination of the optimal radial network configuration is solely driven by reliability. Moreover, for the sake of simplicity, reliability is characterized by four practical reliability indices, namely EENS, SAIFI, SAIDI, and CAIDI. Thus, the network reconfiguration problem at hand is formulated as follows:

$$\text{Minimize } w_E EENS + w_F SAIFI + w_D SAIDI + w_C CAIDI \quad (55)$$

subject to:

$$\text{Expressions (2)–(12), (14)–(23), (25)–(29), (31)–(36), (40), and (44)–(50).} \quad (56)$$

Represented by expression (55), the objective function is the weighted sum of the aforementioned reliability indices. According to Section 3, the mixed-integer linear constraints required to model such reliability indices are

Table 3: Base Instance–Results

Test network	EENS	SAIDI	SAIFI	CAIDI	Objective function
24 nodes	5.208	0.135	0.255	0.530	6.128
54 nodes	10.136	0.704	0.610	1.154	12.604
118 nodes	13.608	0.599	0.729	0.821	15.757

EENS: MWh/year
SAIDI: hours/customer/year
SAIFI: interruptions/customer/year
CAIDI: hours/affected customer/year

included in (56). As an instance of MILP, this model can be efficiently solved by commercially available software based on the branch-and-cut algorithm [33], which not only guarantees finite convergence to the global optimum, but also provides a measure of the distance to optimality over the solution process [34].

5. Numerical Experience

This section is devoted to describing our numerical experience backing the contributions of this paper, namely the consideration of DG, CAIDI, and switching interruptions using an explicit formulation for the topological dependence of distribution reliability assessment. To that end, the reconfiguration problem presented in Section 4 has been solved for three test networks with 24, 54, and 118 nodes. For the sake of reproducibility, network, DG, and demand data for the benchmarks are accessible from [35]. In addition, DG-related results for all case studies are available in [35]. All cases have been implemented using GAMS 27.3 and CPLEX 12.9, on a Dell Precision 3650 Tower PC with a 6 Core 2.80 GHz Intel Core i5-11600 processor and 32 GB of RAM. For all simulations, the optimality tolerance of CPLEX was set at 0%.

5.1. Base Instance

Problem (55)–(56) has been first solved with all weighting factors equal to 1, which required 1.11 s, 232.33 s, and 1,416.11 s for the 24-, 54-, and 118-node systems, respectively. Table 3 presents the reliability indices resulting from this base instance for the three benchmarks. Also, the optimal network topology for the 24-node system is depicted in Fig. 3. Note that, unlike previous works [19–32], the proposed MILP-based approach allows effectively handling all practical reliability indices including the nonlinear and nonconvex relationship between SAIDI and SAIFI featured by CAIDI.

5.2. Impact of DG

In order to illustrate the impact of DG on reliability, the proposed model has also been applied to the passive counterparts of the three test systems, wherein DG units are dropped, as done in [19–21, 23–28, 30–32]. Table 4 presents the resulting values for the reliability indices and the objective function. As can be observed, the reliability of the networks is in general substantially lower compared to the results provided in Table 3 for the corresponding

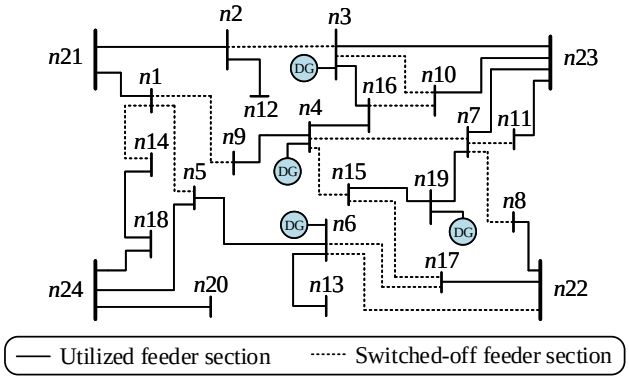

Figure 3: Base instance – Optimal topology for the 24-node network.

Table 4: Base Instance without DG–Results

Test network	EENS	SAIDI	SAIFI	CAIDI	Objective function
24 nodes	5.784	0.153	0.260	0.590	6.787
54 nodes	11.249	0.784	0.610	1.284	13.927
118 nodes	15.779	0.695	0.741	0.938	18.153

EENS: MWh/year
SAIDI: hours/customer/year
SAIFI: interruptions/customer/year
CAIDI: hours/affected customer/year

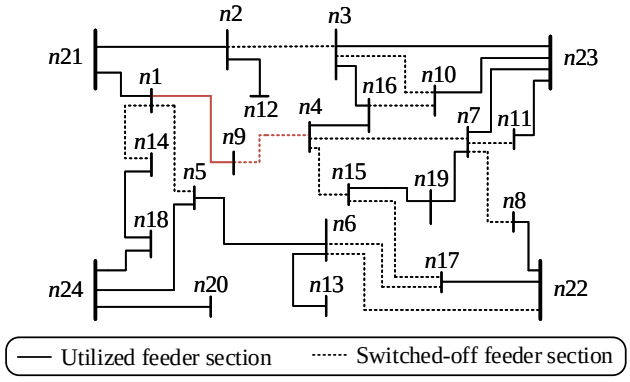

Figure 4: Base instance without DG – Optimal topology for the 24-node network.

active networks. As an exception, SAIFI remains unaltered for the 54-node system. This result stems from the fact that, for this particular benchmark, the proposed model identifies the same optimal network topologies for both the active and passive distribution networks. Fig. 4 shows the optimal topology for the passive 24-node network, where the configuration changes with respect to Fig. 3 are marked with red color. As per this figure, considering the lack of power generation backup by the DG units, load node $n9$ is supplied by the substation located at node $n21$ through a shorter path compared to the topology in Fig. 3. It is worth mentioning that, for the passive networks, we also replaced the proposed formulation for SAIDI, SAIFI, and EENS with that reported in [30], which yielded identical results, as expected.

The impact of DG on the reliability indices has been further assessed by carrying out a sensitivity analysis on

Table 5: Base Instance–Impact of DG Capacity for the 54-Node Network

	Scaling factor				
	0.0	0.5	1.0	1.5	2.0
EENS	11.249	10.674	10.136	9.528	8.964
SAIDI	0.784	0.744	0.704	0.669	0.627
SAIFI	0.610	0.610	0.610	0.657	0.657
CAIDI	1.284	1.219	1.154	1.018	0.954
Objective function	13.927	13.247	12.604	11.872	11.202

EENS: MWh/year
SAIDI: hours/customer/year
SAIFI: interruptions/customer/year
CAIDI: hours/affected customer/year

Table 6: Instance without CAIDI–Results Using the Approximate Model Proposed in [29]

		24 nodes	54 nodes	118 nodes
Approximate results	EENS	2.865	5.366	5.973
	SAIDI	0.078	0.382	0.262
	SAIFI	0.175	0.255	0.104
	Objective function	3.118	6.003	6.339
Actual results	EENS	5.340	10.377	14.173
	SAIDI	0.138	0.723	0.625
	SAIFI	0.289	0.681	0.810
	Objective function	5.767	11.781	15.608

EENS: MWh/year
SAIDI: hours/customer/year
SAIFI: interruptions/customer/year

the DG penetration for the 54-node network. In this respect, DG capacities are multiplied by a scaling factor ranging from 0 to 2 with a step of 0.5. The outcomes for this analysis are presented in Table 5. As per this table, increasing the DG penetration improves the objective function reflecting the overall network reliability. Moreover, as the DG capacity grows, all reliability indices monotonically improve except for SAIFI. Note that SAIFI amounts to 0.610 interruptions/customer/year for scaling factors equal to 0.0, 0.5, and 1.0, and even slightly worsens up to 0.657 interruptions/customer/year when the scaling factor increases to 1.5 and 2.0. Such a single change in SAIFI is associated with the only modification experienced by the optimal network topology resulting along the sensitivity analysis, which occurs when the scaling factor is set to 1.5. This result is consistent with the fact that SAIFI remains unchanged for topologically identical networks no matter how much DG capacities differ since DG has no impact on the number of customer interruptions.

5.3. Importance of Modeling Switching Interruptions

In order to assess the impact of switching interruptions on the reliability indices, we have implemented a modified version of problem (55)–(56) relying on the reliability evaluation technique introduced in [29], wherein switching interruptions are disregarded. In addition, since CAIDI is not modeled in [29], the weighting factor w_C is set to 0. The results provided by the approximate model are listed in Table 6 whereas the optimal topology for the 24-node network is depicted in Fig. 5. To evaluate the

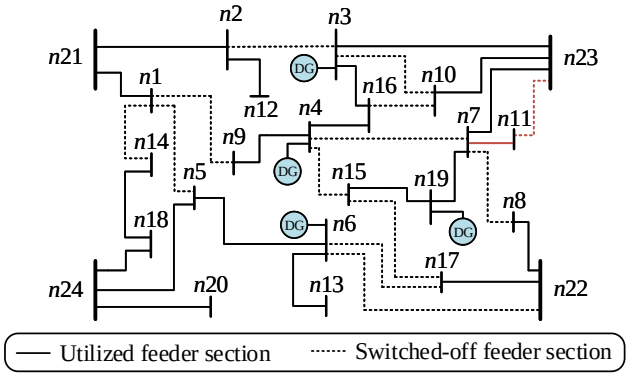

Figure 5: Instance without CAIDI – Optimal topology for the 24-node network using the approximate model proposed in [29].

Table 7: Instance without CAIDI–Results Using the Proposed Model

		24 nodes	54 nodes	118 nodes
	EENS	5.187	10.136	13.608
	SAIDI	0.141	0.704	0.599
	SAIFI	0.260	0.610	0.729
	Objective function	5.588	11.450	14.936
Improvement (%)	EENS	2.865	2.322	3.986
	SAIDI	-2.174	2.628	4.160
	SAIFI	10.035	10.426	10.000
	Objective function	3.104	2.810	4.305

EENS: MWh/year
SAIDI: hours/customer/year
SAIFI: interruptions/customer/year

error caused by disregarding switching interruptions, Table 6 also provides the actual values for the reliability indices and the objective function for the resulting network topologies should the impact of switching interruptions be captured. As can be seen in Table 6, the model presented in [29] substantially underestimates the reliability indices.

Moreover, Table 7 shows the results for the optimal solutions obtained using the proposed reliability model with w_C equal to 0. This table also lists the corresponding improvements upon the actual values reported in Table 6 for the optimal solutions provided by the approximate model developed in [29]. As can be observed, improvements are attained for all indices and networks except for SAIDI for the 24-node grid. Nevertheless, the deterioration of this index is offset by the enhancement of EENS and SAIFI. Thus, as expected, the proposed model yields better solutions in terms of the composite objective function minimized in (55). This result is especially featured for the largest network, for which the impact of switching interruptions is higher.

Lastly, the optimal topology of the 24-node network for the proposed model is shown in Fig. 6, where the differences from Fig. 5 are highlighted in blue. Note that the overall 3.104% improvement reported in Table 7 is attained by modifying the configuration of four feeder sections, namely $n1$-$n9$, $n4$-$n9$, $n7$-$n11$, and $n11$-$n23$.

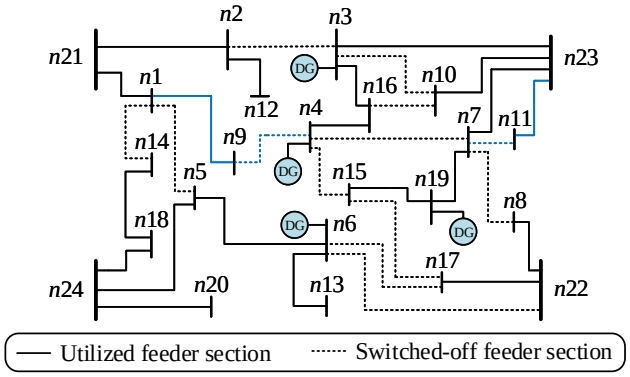

Figure 6: Instance without CAIDI – Optimal topology for the 24-node network using the proposed model.

6. Conclusion

Within the context of explicit formulations for the topological dependence of distribution reliability assessment, this paper has presented a novel approach for active distribution networks. For the first time in the related literature, the effects on reliability of both dispatchable distributed generation and switching interruptions are jointly accounted for. As another salient feature, a precise formulation is devised for CAIDI, which is a practical reliability metric widely used in industry but typically neglected in previous relevant works due to its nonlinearity and nonconvexity. Using a system-oriented framework, the proposed approach is based on mixed-integer linear programming, which allows leveraging well-known convergence properties and the ready availability of effective off-the-shelf software. The proposed reliability assessment can thus be incorporated into the optimization problems customarily solved for reliability-constrained distribution operation and planning, wherein the network topology is unknown a priori. Such a modeling capability is illustrated with a reliability-driven network reconfiguration problem and numerical experience on three test networks. Numerical results reveal 1) the benefits of accurately incorporating dispatchable distributed generation and switching interruptions as compared with state-of-the-art methods, 2) the superior modeling capability of the proposed formulation, as CAIDI is precisely accounted for without resorting to approximate techniques, 3) the computational effectiveness of the proposed approach, and 4) its ability to capture the significant reliability improvements that can be attained by slight differences in the network topology.

Further work will explore the incorporation of the proposed formulation into other practical instances of reliability-constrained distribution network operation and planning. Another interesting avenue of research is the extension of the problem formulation to account for uncertainty sources, including nondispatchable renewable-based distributed generation, through scenario-based stochastic programming, robust optimization, or interval optimization. Research will also be conducted to incorporate the effect of the fault location process and more sophisticated post-fault operational procedures.

References

[1] R. E. Brown, *Electric Power Distribution Reliability*, 2nd ed. Boca Raton, FL, USA: CRC Press, 2008.

[2] U.S. Department of Energy. (2017, Jan.). Quadrennial Energy Review – Transforming the Nation's Electricity System: The Second Installment of the QER. Washington, DC, USA. [Online]. Available: https://www.energy.gov/sites/prod/files/2017/02/f34/Quadrennial%20Energy%20Review--Second%20Installment%20(Full%20Report).pdf

[3] Council of European Energy Regulators. (2018, Jul.). CEER Benchmarking Report 6.1 on the Continuity of Electricity and Gas Supply. Brussels, Belgium. [Online]. Available: https://www.ceer.eu/documents/104400/-/-/963153e6-2f42-78eb-22a4-06f1552dd34c

[4] E. Fumagalli, L. Lo Schiavo, and F. Delestre, *Service Quality Regulation in Electricity Distribution and Retail*. Berlin, Germany: Springer Science & Business Media, 2007.

[5] A. A. Chowdhury and D. O. Koval, *Power Distribution System Reliability: Practical Methods and Applications*, Hoboken, NJ, USA: John Wiley & Sons, 2009.

[6] H. L. Willis, *Power Distribution Planning Reference Book*, 2nd ed. New York, NY, USA: Marcel Dekker, 2004.

[7] R. Billinton and R. N. Allan, *Reliability Evaluation of Power Systems*. New York, NY, USA: Plenum Press, 1984.

[8] B. Sultana, M. W. Mustafa, U. Sultana, and A. R. Bhatti, "Review on reliability improvement and power loss reduction in distribution system via network reconfiguration," *Renew. Sust. Energ. Rev.*, vol. 66, pp. 297–310, Dec. 2016.

[9] K. Xie, J. Zhou, and R. Billinton, "Fast algorithm for the reliability evaluation of large-scale electrical distribution networks using the section technique," *IET Gener. Transm. Distrib.*, vol. 2, no. 5, pp. 701–707, Sep. 2008.

[10] S. Conti, R. Nicolosi, and S. A. Rizzo, "Generalized systematic approach to assess distribution system reliability with renewable distributed generators and microgrids," *IEEE Trans. Power Deliv.*, vol. 27, no. 1, pp. 261–270, Jan. 2012.

[11] S. Conti, S. A. Rizzo, E. F. El-Saadany, M. Essam, and Y. M. Atwa, "Reliability assessment of distribution systems considering telecontrolled switches and microgrids," *IEEE Trans. Power Syst.*, vol. 29, no. 2, pp. 598–607, Mar. 2014.

[12] T. Adefarati and R. C. Bansal. "Reliability assessment of distribution system with the integration of renewable distributed generation," *Appl. Energy*, vol. 185, part 1, pp. 158–171, Jan. 2017.

[13] A. Escalera, M. Prodanović, E. D. Castronuovo, and J. Roldan-Perez, "Contribution of active management technologies to the reliability of power distribution networks," *Appl. Energy*, vol. 267, article no. 114919, Jun. 2020.

[14] R. C. Lotero and J. Contreras, "Distribution system planning with reliability," *IEEE Trans. Power Deliv.*, vol. 26, no. 4, pp. 2552–2562, Oct. 2011.

[15] G. Muñoz-Delgado, J. Contreras, and J. M. Arroyo, "Multistage generation and network expansion planning in distribution systems considering uncertainty and reliability," *IEEE Trans. Power Syst.*, vol. 31, no. 5, pp. 3715–3728, Sep. 2016.

[16] B. R. Pereira, Jr., A. M. Cossi, J. Contreras, and J. R. S. Mantovani, "Multiobjective multistage distribution system planning using tabu search," *IET Gener. Transm. Distrib.*, vol. 8, no. 1, pp. 35–45, Jan. 2014.

[17] F. R. Alonso, D. Q. Oliveira, and A. C. Z. de Souza, "Artificial immune systems optimization approach for multiobjective distribution system reconfiguration," *IEEE Trans. Power Syst.*, vol. 30, no. 2, pp. 840–847, Mar. 2015.

[18] S. Heidari and M. Fotuhi-Firuzabad, "Integrated planning for distribution automation and network capacity expansion," *IEEE Trans. Smart Grid*, vol. 10, no. 4, pp. 4279–4288, Jul. 2019.

[19] J. C. López, M. Lavorato, and M. J. Rider, "Optimal reconfiguration of electrical distribution systems considering reliability indices improvement," *Int. J. Electr. Power Energy Syst.*, vol. 78, pp. 837–845, Jun. 2016.
[20] G. Muñoz-Delgado, J. Contreras, and J. M. Arroyo, "Reliability assessment for distribution optimization models: A non-simulation-based linear programming approach," *IEEE Trans. Smart Grid*, vol. 9, no. 4, pp. 3048–3059, Jul. 2018.
[21] G. Muñoz-Delgado, J. Contreras, and J. M. Arroyo, "Distribution network expansion planning with an explicit formulation for reliability assessment," *IEEE Trans. Power Syst.*, vol. 33, no. 3, pp. 2583–2596, May 2018.
[22] R. Wu and G. Sansavini, "Integrating reliability and resilience to support the transition from passive distribution grids to islanding microgrids," *Appl. Energy*, vol. 272, article no. 115254, Aug. 2020.
[23] A. Tabares, G. Muñoz-Delgado, J. F. Franco, J. M. Arroyo, and J. Contreras, "An enhanced algebraic approach for the analytical reliability assessment of distribution systems," *IEEE Trans. Power Syst.*, vol. 34, no. 4, pp. 2870–2879, Jul. 2019.
[24] Z. Li, W. Wu, B. Zhang, and X. Tai, "Analytical reliability assessment method for complex distribution networks considering post-fault network reconfiguration," *IEEE Trans. Power Syst.*, vol. 35, no. 2, pp. 1457–1467, Mar. 2020.
[25] Z. Li, W. Wu, X. Tai, and B. Zhang, "Optimization model-based reliability assessment for distribution networks considering detailed placement of circuit breakers and switches," *IEEE Trans. Power Syst.*, vol. 35, no. 5, pp. 3991–4004, Sep. 2020.
[26] Z. Li, W. Wu, B. Zhang, and X. Tai, "Feeder-corridor-based distribution network planning model with explicit reliability constraints," *IET Gener. Transm. Distrib.*, vol. 14, no. 22, pp. 5310–5318, Nov. 2020.
[27] Z. Li, W. Wu, X. Tai, and B. Zhang, "A reliability-constrained expansion planning model for mesh distribution networks," *IEEE Trans Power Syst.*, vol. 36, no. 2, pp. 948–960, Mar. 2021.
[28] M. Jooshaki, A. Abbaspour, M. Fotuhi-Firuzabad, H. Farzin, M. Moeini-Aghtaie, and M. Lehtonen, "A MILP model for incorporating reliability indices in distribution system expansion planning," *IEEE Trans. Power Syst.*, vol. 34, no. 3, pp. 2453–2456, May 2019.
[29] M. Jooshaki, A. Abbaspour, M. Fotuhi-Firuzabad, M. Moeini-Aghtaie, and M. Lehtonen, "MILP model of electricity distribution system expansion planning considering incentive reliability regulations," *IEEE Trans. Power Syst.*, vol. 34, no. 6, pp. 4300–4316, Nov. 2019.
[30] M. Jooshaki, A. Abbaspour, M. Fotuhi-Firuzabad, G. Muñoz-Delgado, J. Contreras, M. Lehtonen, and J. M. Arroyo, "Linear formulations for topology-variable-based distribution system reliability assessment considering switching interruptions," *IEEE Trans. Smart Grid*, vol. 11, no. 5, pp. 4032–4043, Sep. 2020.
[31] M. Jooshaki, M. Lehtonen, M. Fotuhi-Firuzabad, G. Muñoz-Delgado, J. Contreras, and J. M. Arroyo, "Optimization-based distribution system reliability evaluation: An enhanced MILP model," presented at the Int. Conf. Smart Energy Syst. Technol. (SEST), Vaasa, Finland, Sep. 6–8, 2021.
[32] M. Jooshaki, A. Abbaspour, M. Fotuhi-Firuzabad, G. Muñoz-Delgado, J. Contreras, M. Lehtonen, and J. M. Arroyo, "An enhanced MILP model for reliability-constrained distribution network expansion planning," *IEEE Trans. Power Syst.*, vol. 37, no. 1, pp. 118–131, Jan. 2022.
[33] IBM ILOG CPLEX, 2022. [Online] Available: https://www.ibm.com/analytics/cplex-optimizer
[34] G. L. Nemhauser and L. A. Wolsey, *Integer and Combinatorial Optimization*. New York, NY, USA: Wiley-Interscience, 1999.
[35] M. Jooshaki, M. Lehtonen, M. Fotuhi-Firuzabad, G. Muñoz-Delgado, J. Contreras, and J. M. Arroyo, "On the explicit formulation of reliability assessment of distribution systems with unknown network topology: Incorporation of DG, switching interruptions, and customer-interruption quantification – Data and results for the case studies," Mendeley Data, V3. [Online]. Available: https://data.mendeley.com/datasets/c86fsh79m9/3. Accessed: Jun. 2022.